



Published in final edited form as:

*Pain*. 2014 December ; 155(12): 2502–2509. doi:10.1016/j.pain.2014.09.002.

## Preliminary structural MRI based brain classification of chronic pelvic pain: A MAPP Network Study

Epifanio Bagarinao, PhD<sup>1</sup>, Kevin A. Johnson, RN PhD<sup>1</sup>, Katherine T. Martucci, PhD<sup>1</sup>, Eric Ichesco<sup>4</sup>, Melissa A. Farmer, PhD<sup>5</sup>, Jennifer Labus, PhD<sup>2</sup>, Timothy J. Ness, MD, PhD<sup>3</sup>, Richard Harris, PhD<sup>4</sup>, Georg Deutsch, PhD<sup>3</sup>, A. Vania Apkarian, PhD<sup>5</sup>, Emeran A. Mayer, MD<sup>2</sup>, Daniel J. Clauw, MD<sup>4</sup>, and Sean Mackey, MD PhD<sup>1</sup>

<sup>1</sup>Department of Anesthesiology, Perioperative and Pain Medicine, Division of Pain Medicine, Stanford University Medical Center, Stanford, CA, USA

<sup>2</sup>Gail and Gerald Oppenheimer Family Center for Neurobiology of Stress, Pain and Interoception Network (PAIN), David Geffen School of Medicine at UCLA, Los Angeles, CA, USA

<sup>3</sup>Departments of Radiology and Anesthesiology, University of Alabama, Birmingham Medical Center, USA

<sup>4</sup>Department of Anesthesiology, Chronic Pain and Fatigue Research Center, University of Michigan, Ann Arbor, MI, USA

<sup>5</sup>Department of Physiology, Northwestern University, Feinberg School of Medicine, 303 E. Chicago Avenue, Chicago, IL, USA

### Abstract

Neuroimaging studies have shown that changes in brain morphology often accompany chronic pain conditions. However, brain biomarkers that are sensitive and specific to chronic pelvic pain (CPP) have not yet been adequately identified. Using data from the Trans-MAPP Research Network, we examined the changes in brain morphology associated with CPP. We used a multivariate pattern classification approach to detect these changes and to identify patterns that could be used to distinguish participants with CPP from age-matched healthy controls. In particular, we used a linear support vector machine (SVM) algorithm to differentiate gray matter images from the two groups. Regions of positive SVM weight included several regions within the primary somatosensory cortex, pre-supplementary motor area, hippocampus, and amygdala were identified as important drivers of the classification with 73% overall accuracy. Thus, we have identified a preliminary classifier based on brain structure that is able to predict the presence of CPP with a good degree of predictive power. Our regional findings suggest that in individuals

---

**Corresponding Author:** Sean Mackey, M.D., Ph.D., Redlich Professor, Departments of Anesthesiology, Perioperative and Pain Medicine | Neurosciences | Neurology (by courtesy), Chief, Division of Pain Medicine, Director, Stanford Systems Neuroscience and Pain Lab (SNAPL), Stanford University School of Medicine, 1070 Arastradero Road, Room 285, MC 5596, Palo Alto, CA 94304-1336, Ph: (650) 498-6477 | Fx: (650) 725-9642 | smackey@stanford.edu.

**Publisher's Disclaimer:** This is a PDF file of an unedited manuscript that has been accepted for publication. As a service to our customers we are providing this early version of the manuscript. The manuscript will undergo copyediting, typesetting, and review of the resulting proof before it is published in its final citable form. Please note that during the production process errors may be discovered which could affect the content, and all legal disclaimers that apply to the journal pertain.

The authors declare no conflicts of interest.

with CPP, greater gray matter density may be found in the identified distributed brain regions, which are consistent with some previous investigations in visceral pain syndromes. Future studies are needed to improve upon our identified preliminary classifier with integration of additional variables and to assess whether the observed differences in brain structure are unique to CPP or generalizable to other chronic pain conditions.

## Keywords

gray matter density; machine learning; support vector machine; SVM; UCPPS

---

## Introduction

Chronic pelvic pain (CPP) affects approximately 3–6 % of women in the United States, impacts the quality of life, reduces work productivity, and adds financial burden to the health care system [10, 31]. Individuals with CPP typically experience a combination of both pain (e.g. constant and/or evoked), without specific etiology (e.g. no observable pathology) localized in the pelvic region, and urinary symptoms (e.g. urgency and increased frequency) by definition lasting for at least 3 months. Similar to other chronic pain conditions, little is known about the mechanisms underlying CPP, and its pathogenesis is still not fully understood [31].

To counter the great lack of understanding and knowledge pertaining to the etiology and prognosis of CPP, a multi-site study, the U.S. NIH MAPP Research Network was formed ([www.mappnetwork.org](http://www.mappnetwork.org)). Due to the lack of effective biomarkers for CPP, the Neuroimaging Working Group of the MAPP Research Network was formed with a goal of developing neuroimaging-based biomarkers for CPP.

Recent neuroimaging studies have shown that changes in brain morphology often accompany chronic pain conditions [3, 4, 8, 16, 32, 50, 57] especially affecting areas related to pain perception and modulation. Historically, these changes in regional gray matter volume have been detected using mass univariate methods such as voxel based morphometry (VBM), where differences in group intensities are tested for statistical significance for each volume element (voxel) (for review [5]). However, these differences in gray matter may ultimately reflect a distributed network of altered brain regions, and univariate techniques are often not able to capture the specific distributed spatial patterns. Newer approaches using multivariate pattern analysis (MVPA) are able to characterize the spatially distributed and covarying patterns of brain activity and structure and are yielding rich information about underlying conditions (for review, see [39]). In addition to providing greater mechanistic information, MVPA approaches provide classification metrics such as accuracy, sensitivity, and specificity that can be useful in translating the results into a clinically useful biomarker.

One form of the MVPA approach uses support vector machine (SVM). SVM algorithms are effective in discriminating patterns of brain activity and structure that occur in neurodegenerative diseases and mental disorders [9, 19]. We [12] and others [56] have recently demonstrated an SVM algorithm's effectiveness to classify acute pain. We have

also used an SVM algorithm to classify brain images from participants with chronic low back pain from that of healthy controls with high classification accuracy of 75%. Others have classified chronic low back pain using measures of brain functional connectivity [2, 53].

As part of the MAPP Research Network, we captured a large set of structural MRI data from female participants with CPP and age-matched, female healthy controls. Our overall goals in this study were: (1) to identify a multivariate structural brain classifier coinciding with CPP using an SVM algorithm, and (2) to assess the accuracy of this brain classifier in discriminating CPP from healthy controls. We also investigated relationships between brain structure in CPP versus symptom duration, symptom severity, and psychological measures.

## Materials and Methods

### Participants

Data from the MAPP Research Network neuroimaging study were used [15]. These data were collected through a uniform and collaborative effort across multiple neuroimaging sites including Stanford University, University of California Los Angeles, University of Alabama at Birmingham, University of Michigan, Northwestern University and University of Washington. All study participants provided signed written consent that they understood and were willing to undergo the procedures of the study, which had been approved in accordance with the Institutional Review Board at the participant's site of involvement in the study. The dataset consisted of structural images from 33 female participants with chronic pelvic pain and 33 age and gender matched healthy controls. All participants were extensively characterized as part of the TransMAPP Research Network Protocol which included an initial 4 hour visit (eligibility screening, 2 urine samples, a blood draw, and extensive online module questionnaires to provide phenotype data), and an MRI scan visit scheduled within 24 hours of the initial baseline visit [29]. Participants with CPP were also asked to continue with biweekly and bimonthly questionnaires, return for a 6 month and 12 month in-person follow-up visit. (Non-neuroimaging data to be published as separate manuscripts.) The average ( $\pm$  standard deviation) age for the patient group was 39.51 ( $\pm$ 12.09) years, while for the healthy control group was 38.95 ( $\pm$  11.64) years. For the patient group, the average symptom duration was 9.09 ( $\pm$  9.79) years, with the longest duration being 32.11 years and the shortest 0.57 years. Participants were included on the basis of having no other major somatic symptoms (e.g. fibromyalgia, irritable bowel syndrome, chronic fatigue syndrome). However, of the participants included, 7 reported symptoms of vulvodynia and 8 reported symptoms of temporomandibular disorders. In terms of medications used, 6 participants were taking opioid medications, 7 were taking centrally acting pain medications (antidepressants, benzodiazepines, anticonvulsants, immunosuppressant drugs), 11 were taking peripherally acting pain medications (e.g. NSAIDs) and 9 participants were taking no medications for pain.

### Questionnaires

Several questionnaires were administered prior to the MRI scan session including the McGill Pain Questionnaire (MPQ) and the Hospital Anxiety and Depression Scale (HADS).

From the MPQ a total sensory score was used to assess the correlation of pain intensity with GM density. From the HADS, anxiety and depression total scores were used to assess the correlation of psychological state with GM density.

### Image acquisition

Trans-MAPP neuroimaging data was collected, quality controlled and archived according to multi site imaging procedures developed collaboratively between the MAPP Research Network, the UCLA PAIN repository and the UCLA Laboratory of Neuroimaging (LONI). Detailed procedures and description of the repository are available at [painrepository.org](http://painrepository.org). Scanner compatible acquisition parameters were developed and all sites were required to complete and pass a site qualification including a set of pilot scans of a human volunteer; the initial scans were reviewed for quality control by the UCLA site, and recommendations and adjustments were made as necessary prior to commencement of study scans. Following quality control approval, the same MRI scanner that was used for site qualification was used to acquire all subsequent subject scans at each site, along with the same 8-channel head coil throughout the duration of the study. Scanner upgrades required requalification of the scanners.

All structural T1-weighted images were acquired using a 3D MP-RAGE pulse sequence (Magnetization Prepared Rapid Acquisition Gradient Echo, Siemens) [36] or the equivalent FSPGR IR pulse sequence (Fast SPOiled GRAdient Echo – Inversion Recovery, General Electric, GE). The specific standardized parameters were as follows: TR = 2200 ms, TE = minimum, TI = 750 ms, flip angle = 20 degrees, FoV = 220 mm × 220 mm, resolution = 256 × 256, slices per volume = 176, slice thickness = 1mm, voxel size = 0.86 × 0.86 × 1 mm, slice selective inversion, phased array acceleration factor = 2, phase encode direction = left-right and superior-inferior, orientation = axial-oblique parallel to the line between the anterior and posterior commissures.

Structural images were uploaded to a centralized database at UCLA's PAIN repository where they were run through a thorough automated quality control pipeline; scans that passed quality control standards were then available for download by any of the TransMAPP neuroimaging sites. Quality control standards required for inclusion of structural images included the following criteria: 1. Compliance with acquisition protocol, 2. Full brain coverage, 3. Minimal motion (Gibbs ringing), 4. Absence of Flow/Zipper, 5. Minor Atrophy/Vascular Degeneration (all assessed qualitatively by trained expert at UCLA). Prior to data analysis, we at our site additionally conducted visual, non-automated inspection and quality control of the structural MRI data.

### Image preprocessing

We analyzed T1-weighted structural images from all subjects using SPM8 (Wellcome Trust Center for Neuroimaging, <http://www.fil.ion.ucl.ac.uk/spm/software/spm8/>) running on MATLAB 7 (R2011b). The images were segmented into gray matter (GM), white matter (WM), and cerebrospinal fluid (CSF) components using SPM8's unified segmentation [6]. The segmentation was set to output component images in both native and MNI template space. The normalized and modulated GM images were then spatially smoothed using an 8

mm full width at half maximum Gaussian filter. These pre-processed GM images were then used in the SVM algorithm based analysis.

### Support vector machine (SVM) classification

For multivariate pattern classification, we used an SVM algorithm. SVM is a supervised learning algorithm, which requires training examples to generate a classification model for a given problem [43]. In particular, the SVM algorithm attempts to determine a separating hyperplane (decision boundary) optimizing the separation between two groups. After training, the decision boundary can be used to classify datasets not yet seen by the SVM algorithm. It can also be used to determine features that significantly contribute to the classification process. In the current context, SVMs were trained to classify GM images as either belonging to participants with chronic pelvic pain (assigned class value of +1) or healthy controls (class value of -1). Each voxel in the image was treated as a feature and each GM image represented a point in a high-dimensional feature space. Using available dataset, SVM algorithms were then trained to obtain a hyperplane optimally separating the images from the two groups. To minimize the dimensionality of the feature space and ensure that we were only investigating GM, we included only voxels in the GM image with values greater than 0.1. We used a linear SVM algorithm and set the regularization parameter to 1.

Decreases in GM density are known to occur with increasing age [37, 41]. Therefore, because the ages among our groups were somewhat variable, and because we did not want age as a driving input for our classification, we regressed out age from the data before SVM classification analyses. Site-related differences in GM density were also regressed from the analysis through adjustment of mean GM intensity values as follows. For each voxel in a given image, a correction factor was applied [mean intensity over all GM images from the image's site (site mean) minus mean intensity over all voxels from all images included in the analysis (global mean)].

In the absence of a proper test set to evaluate the classification performance of the trained SVM, we used a leave-one-out cross validation (LOOCV) approach. LOOCV provides a relatively unbiased estimate of the classifier's true generalization performance [1]. In this approach, GM images from all but one subject ( $N-1$  of the  $N$  subjects) are used for training the SVM. The trained SVM is then tested using the remaining image. This process is repeated until all the images are used as a test image. The LOOCV classification accuracy is calculated as the percentage of images that are correctly classified. The alternative approach of leave-pair-out cross validation (LPOCV) was also tested, despite the limitation that patients and controls were not strictly age matched for each pair (age matching was  $\pm 5$  years for each pair and balanced so that group means were not significantly different). Since there were several possible pair combinations, the LPOCV classification was repeated 1000 times, each time randomizing the pairing of subjects, and the mean classification accuracy was computed.

Aside from the classification accuracy, we also calculated the following classification measures: sensitivity =  $TP / (TP + FN)$ , specificity =  $TN / (TN + FP)$ , positive predictive value  $PPV = TP / (TP + FP)$ , and negative predictive value  $NPV = TN / (TN + FN)$ . TP was defined as the number of images correctly classified as belonging to the patient group (true

positive), TN was defined as the number of images correctly classified as belonging to the healthy control group (true negative), FP was defined as the number of images from the healthy control group misclassified as belonging to the patient group (false positives), and FN was defined as the number of images from the patient group misclassified as belonging to the healthy control group (false negative). All of these additional values were assessed for significance level using permutation tests following [53].

For this analysis, we used a MATLAB version of LIBSVM, a library for support vector machines (<http://www.csie.ntu.edu.tw/~cjlin/libsvm>, [14]).

### Permutation Test

We were also interested in the significance of each voxel's contribution to the classification accuracy. We used a permutation test [35] with 5000 iterations to generate an SVM-derived significance map, a map showing regions that significantly contributed to the classification performance of the trained SVM. In brief, this nonparametric test involved randomly permuting the class labels and training an SVM for each permutation. This gives an estimate of the probability distribution of the SVM weight associated with each voxel under the null hypothesis of no relationship between class labels and the global structure of the training data. The p-value is then calculated as the proportion of values in the null distribution that is greater or equal to the value obtained using the original (i.e. non-permuted) labels. Thus, the farther away the weight value of a voxel from the major mass of the distribution under null hypothesis (small p-value), the more likely it is to be significantly predictive for the class label. The significance map was corrected for multiple comparisons using false discovery rate with  $q < 0.05$  and cluster size greater than 20 voxels. We used an SPM8 extension, *xjview* (<http://www.alivelearn.net/xjview8>), for the anatomical labeling of significant brain regions.

Using the same approach, we also estimated the significance of the classification accuracy and other classification measures described above. For each permutation, we computed the LOOCV / LPOCV accuracy, sensitivity, and specificity, among others. The p-value associated with each measure was calculated as the proportion of values in the null distribution greater than the value obtained when using the nonpermuted labels.

### ROI correlation analysis

Several regions of interest (ROIs) were extracted from the significance map. The values of the GM density from all voxels within each ROI were extracted from patient data sets and the mean computed. The correlation of the ROI's mean density with other behavioral measures (symptom severity, pain duration, anxiety and depression) across all CPP patients was estimated. Previously, brain morphological changes were observed as correlating with duration of chronic pain symptoms, but only when the patient population was split into subgroups and separately assessed for short (< 5 years) or long-term (> 5 years) symptom duration [8]. Therefore, we similarly wished to investigate the relationship of our inferred GM density change with chronic pain duration at different stages of chronic pain. Due to our initially observed overall non-linear relationship of duration and GM density, we used a systematic approach to characterize the correlations of duration subsets. To do this, we



partitioned the range of symptom duration into two intervals – from 0 to  $x$  and  $x$  to 33 (greatest symptom duration in our population, years) and systematically varied  $x$  from 2.5, 5.0, 7.5, and 10. The correlation of GM density with symptom duration for each interval was then computed.

### Total GM volume

We also performed statistical analysis of the total GM volume. Total GM volume was computed by multiplying the value of each voxel by its total volume and summing over all voxels included. A two-sided two-sample t-test was used to determine if the difference of mean total gray matter volume between the two groups was significant. Total whole brain GM volume values were also entered into an additional SVM analysis to test whether total GM volume could predict CPP from healthy controls.

## Results

The trained SVM performed significantly better than chance in classifying the patient group from the healthy control group (Table 1). The classifier's accuracy when using LOOCV was 72.73% ( $p = 0.039$ ). The sensitivity was 69.70% ( $p = 0.067$ ) and the specificity was 72.73% ( $p = 0.046$ ). The positive and negative predictive values were 71.88% ( $p = 0.039$ ) and 70.59% ( $p = 0.047$ ), respectively. The classifier's accuracy was slightly lower when using LPOCV at 69.36% ( $p = 0.017$ ). The sensitivity was 70.22% ( $p = 0.013$ ) and the specificity was 68.65% ( $p = 0.025$ ). The positive and negative predictive values were 67.41% ( $p = 0.049$ ) and 71.32% ( $p = 0.017$ ), respectively. All following reported results are from the LOOCV analysis.

The classification of individual GM images was visualized by showing the distance of each GM image from the trained SVM's separating hyperplane (Fig. 1A). Positive distance represents patient group (+1) classification, while negative distance represents healthy control group (-1). Participants with negative distance indicate false negatives, while healthy participants with positive distance are false positives.

Several regions of greater GM density were observed in CPP compared to the healthy control group. These regions contributed significantly to the classification performance of the trained SVM to discriminate between brain structure of CPP and healthy controls (Fig. 2). Regions of positive SVM weights included bilateral primary somatosensory cortex (S1), left pre supplementary motor area (pre-SMA), bilateral hippocampus and left amygdala. All regions were corrected for multiple comparisons (FDR,  $q < 0.05$ ) and cluster size greater than 20 voxels. (See Table 2 for the complete list of regions and MNI coordinates.)

Values of GM density within the patient group, from the identified discriminative ROIs (positive SVM weights, which suggest greater regional GM density in the CPP group), were correlated with patients' behavioral measures from the questionnaire data. Pain intensity (MPQ, total sensory score) was significantly correlated with the weights of the left postcentral gyrus/paracentral lobule ( $r = 0.37$ ,  $p = 0.05$ ), left pre-SMA ( $r = 0.38$ ,  $p = 0.05$ ), and right S1 ( $r = 0.55$ ,  $p = 0.0015$ ) (with age regressed out). Depression score (HADS) was

significantly correlated with the weight of the right hippocampus ( $r = 0.36, p = 0.04$ ). Anxiety score (HADS) was not significantly correlated with any region.

As assessed in patients only, symptom duration was not linearly related to any of the identified regions of positive weights contributing to the SVM. However, when limiting the analysis to within specific ranges of symptom duration, some correlations emerged in 4 regions (Figure 3). Specifically, bilateral S1 (both left and right S1 regions) showed a strong positive relationship with durations from 0 to 2.5 years and a significant negative correlation with symptom durations greater than 5 years. In contrast, the left hippocampus was negatively correlated with symptom durations less than 10 years. The left amygdala was significantly correlated with symptom duration less than 7.5 years. (See Table 3 for details.)

Total GM volume was significantly greater in CPP as compared with healthy controls ( $p = 0.0042$ ). SVM classification based on only total GM volume resulted in classification accuracy of 66.67% (with age regressed).

## Discussion

We have identified a preliminary brain classifier associated with CPP. This GM classifier distinguishes individuals with CPP from matched healthy controls with an accuracy of 73%. Based on our findings, several brain regions were revealed to have positive weights contributing to the SVM classification of CPPs versus HCs. These regions included bilateral primary somatosensory cortex (S1), left pre-supplementary motor area (pre-SMA), bilateral hippocampus and left amygdala. The nature of positive weights of these regions suggests that patients with CPP may have increased gray matter density within these regions.

Previous morphological studies of chronic pain have revealed altered (typically decreased) GM density across numerous brain regions implicated in pain processing and perception (for review: [51]). Increased GM density in S1 was observed in another chronic visceral pain syndrome (IBS), both in terms of GM volume [28] and cortical thickness [24]. A region we identified within the primary somatosensory cortex (S1) was highly similar in location to a VBM study of females with CPP also collected through the MAPP Research Network [25]. Somatotopically, two regions that we observed in S1 were within a region activated during electrical stimulation of the human clitoris [33]. Our results of another S1 region (MNI: 44, -24, 56) closely corresponded to a region of S1 activity related to spontaneous pain ratings observed in a previous VBM study of males with chronic pelvic pain (MNI: 36, -28, 58) [21]. Importantly, patients included in our study had symptoms characteristic of interstitial cystitis, with pain in the lower abdomen accompanied by urinary symptoms (e.g. increased urgency, increased frequency of urination, painful filling of the bladder). Also, the majority (85%) of participants with CPP also showed signs of pelvic floor dysfunction, which typically involves a hypertonic state of the pelvic floor musculature [13, 40]. The differences in symptoms between our CPP patient population and those of previous morphological studies of CPP may account for differences in GM density findings. Specifically, one previous CPP study observed decreased GM density within the left middle frontal gyrus, right putamen, bilateral mid-cingulate cortex, right insular cortex, and left thalamus in a patient population with endometriosis and pain. However, these findings of regional



decreased GM density may contrast with our present findings because they defined CPP as moderate to severe pelvic pain greater than or equal to a 4 (10-point scale) and excluded patients with interstitial cystitis [4]. Further, our patient population included only 9 individuals with endometriosis. In contrast to our present findings, and possibly due to sex-related differences in CPP, male CPP patients previously demonstrated decreased GM volume within the left anterior cingulate cortex [34]. Another VBM study of CPP in males, revealed through a region of interest correlation analysis, showed a positive correlation of right insular cortex GM density with pain severity and a positive correlation of anterior cingulate cortex GM density with duration of pain (i.e. pain chronicity) [21].

Positive weights within bilateral parahippocampal / hippocampal gyri and amygdala also significantly contributed to our classification of CPP. Complementary to our findings, greater GM density within the left amygdala was previously observed in a patient population of chronic pelvic pain and endometriosis [4]. However, decreased amygdala GM volume has been observed in IBS [28] and in healthy individuals with increased visceral sensitivity [20]. Increased GM density within the parahippocampal gyrus and basal ganglia has also been observed in participants with provoked vestibulodynia [49]. Increased GM volume has also been observed in patients with primary dysmenorrhea in the right posterior hippocampus among several other brain regions of altered GM volume [52]. In contrast, other studies using VBM have shown less GM in the hippocampus in post-traumatic stress disorder [11, 22, 55] and chronic fatigue syndrome [45]. The amygdala and hippocampus, in addition to processes of emotion and memory, play direct roles in pain modulation and processing of anxiety, fear and aversive contents of pain [17, 30, 38, 42, 44, 48]. Together, our and others' observations of altered GM density within the hippocampus and amygdala in chronic pain states may reflect an altered state of pain modulation and emotional-regulatory aspects of chronic pain.

### **Correlations of Gray Matter Density Change with Symptom Duration**

The range of symptom durations included in each study population could account for inconsistent findings of GM density change. In support of this concept, we observed that the degree of patients' positive SVM weight within regions of our significance map was related to symptom duration, but only at certain stages of chronic pain. This suggests that the relationship between GM density and symptom duration may not be linear over time. Additionally, this relationship differs for distinct brain regions. For example, our results suggest that in S1, GM density may increase in the first few years of chronic pain; but as pain persists past the first initial years, the GM density may decrease – the longer the pain, the less the GM density. In contrast, in the left hippocampus we observed a negative correlation of GM density and symptom duration during the first 10 years of pain but not after (potential decreases in GM density over time up to 10 years), similar to a previous investigation [54]. In other chronic pain conditions, less GM density is observed in insular cortex, S1 and motor cortex; these differences are significantly correlated with pain duration, but only when the duration is greater than 5 years [8]. However, importantly, these observations are not based on longitudinal studies, but rather on correlation results at a single time point. While it currently remains unclear whether chronic pain causes nonlinear

morphological changes over time, emerging data from longitudinal studies indicate that this might be the case [23, 46].

### Enhanced Potential of fMRI Analyses by Using Multivariate Methods

In the present study, through using SVM algorithms, we were able to classify between CPP and healthy controls based on brain morphological differences. Additionally, through our use of the SVM algorithm, we identified several brain regions of positive contributory weights, suggesting greater GM density in these regions in CPP. Some of these regions were in agreement with regions identified in a conventional VBM analysis also conducted through the MAPP Research Network [25]. Compared to the conventional univariate analysis, our SVM approach appeared to be more sensitive to identifying additional regions of morphological differences between CPP and healthy controls. This was somewhat expected due to known increases in power when using multivariate analyses [39] and because we previously observed increased sensitivity when using SVM to classify structural differences in chronic low back pain, as compared with conventional VBM analysis [53].

### Limitations

Brain morphological changes in chronic pain typically show decreases in GM density in brain regions related to aspects of pain processing (for review: [51]). In contrast, our observations of positive SVM weights indicate increased GM density within regions of S1, hippocampus and amygdala in CPP. Thus, changes in brain morphology may vary between different types of chronic pain, as noted previously [7]. For example, less total GM volume is observed in chronic low back pain and fibromyalgia [27], but not in participants with complex regional pain syndrome or knee osteoarthritis. However, regions of increased GM density are not entirely rare. For example, increased GM density has also been observed in striatal regions in fibromyalgia [47, 53]. Differences in directionality of GM change across studies of chronic pain could be attributed to the differences in the various populations being studied, presence or absence of co-morbidities, and medication usage.

We here describe a preliminary structural MRI classifier of CPP. Future characterization of a true brain classifier for CPP will require larger sample sizes, refined models and extensive model validation (e.g., prospective testing and / or inclusion of independent training and test sets). Future analyses could also use more optimal analysis methods of modeled correction for nuisance features such as age [18, 26]. Further, it is currently unknown whether these regions of greater GM density may be a specific feature of CPP and or generalizable to other chronic pain conditions.

### Conclusion

We have identified a preliminary structural brain based classifier representative of CPP. The classifier was comprised of several distributed regions of positive SVM weight that contributed to our SVM algorithm including S1, pre-SMA, the hippocampus and amygdala. While previous studies have typically observed decreased GM density in chronic pain, the regions we identified suggest regional increased GM density in CPP. Ultimately, the good classification accuracy observed in our study suggests the significance of these regions in

distinguishing participants with CPP from healthy controls and serve as a preliminary potential biomarker for CPP. While a structural brain classifier of CPP as a definitive marker of disease would have significant ethical and legal implications, our results are preliminary and further investigation is warranted. Through the combination of SVM analyses of brain structure and function with additional genotype and phenotype biomarkers, we may ultimately define strong predictors of treatment response, define subgroups of chronic pain syndromes and develop tailored and systematic therapy for the individual patient.

## Acknowledgments

Thanks to Cody Ashe-McNally for his technical expertise in coordinating and running the cross-site quality control of all MAPP Research Network neuroimaging data. Special thanks to Jeff Alger for his expertise as a physicist at UCLA in oversight and coordination of the multi-site collection of neuroimaging data. This study was supported by the NIH NIDDK / UPenn U01 DK082316, NS05391, NS048302, K24 DA029262 and Redlich Pain Research Endowment.

## References

1. Airola A, et al. An experimental comparison of cross-validation techniques for estimating the area under the ROC curve. *Computational Statistics & Data Analysis*. 2011; 55(4):1828–1844.
2. Apkarian AV, Baliki MN, Farmer MA. Predicting transition to chronic pain. *Current Opinion in Neurology*. 2013; 26(4):360–367. [PubMed: 23823463]
3. Apkarian AV, et al. Chronic back pain is associated with decreased prefrontal and thalamic gray matter density. *Journal of Neuroscience*. 2004; 24(46):10410–10415. [PubMed: 15548656]
4. As-Sanie S, et al. Changes in regional gray matter volume in women with chronic pelvic pain: A voxel-based morphometry study. *Pain*. 2012; 153(5):1006–1014. [PubMed: 22387096]
5. Ashburner J, Friston KJ. Voxel-based morphometry - The methods. *Neuroimage*. 2000; 11(6):805–821. [PubMed: 10860804]
6. Ashburner J, Friston KJ. Unified segmentation. *Neuroimage*. 2005; 26(3):839–851. [PubMed: 15955494]
7. Baliki MN, et al. Brain morphological signatures for chronic pain. *PLoS One*. 2011; 6(10):e26010. [PubMed: 22022493]
8. Baliki MN, et al. Brain Morphological Signatures for Chronic Pain. *Plos One*. 2011; 6(10)
9. Bendfeldt K, et al. Multivariate pattern classification of gray matter pathology in multiple sclerosis. *Neuroimage*. 2012; 60(1):400–408. [PubMed: 22245259]
10. Berry SH, et al. Prevalence of Symptoms of Bladder Pain Syndrome/Interstitial Cystitis Among Adult Females in the United States. *Journal of Urology*. 2011; 186(2):540–544. [PubMed: 21683389]
11. Bremner JD, et al. Mri-Based Measurement of Hippocampal Volume in Patients with Combat-Related Posttraumatic-Stress-Disorder. *American Journal of Psychiatry*. 1995; 152(7):973–981. [PubMed: 7793467]
12. Brown JE, et al. Towards a Physiology-Based Measure of Pain: Patterns of Human Brain Activity Distinguish Painful from Non-Painful Thermal Stimulation. *Plos One*. 2011; 6(9)
13. Butrick CW. Interstitial cystitis and chronic pelvic pain: new insights in neuropathology, diagnosis, and treatment. *Clin Obstet Gynecol*. 2003; 46(4):811–823. [PubMed: 14595223]
14. Chang CC, Lin CJ. LIBSVM: A Library for Support Vector Machines. *Acem Transactions on Intelligent Systems and Technology*. 2011; 2(3)
15. Clemens JQ, et al. The MAPP research network: a novel study of urologic chronic pelvic pain syndromes. *BMC Urol*. 2014; 14(1):57. [PubMed: 25085007]
16. Davis KD, et al. Cortical thinning in IBS: Implications for homeostatic, attention, and pain processing. *Neurology*. 2008; 70(2):153–154. [PubMed: 17959767]

17. Derbyshire SWG, et al. Pain processing during three levels of noxious stimulation produces differential patterns of central activity. *Pain*. 1997; 73(3):431–445. [PubMed: 9469535]
18. Dukart J, Schroeter ML, Mueller K. Age correction in dementia--matching to a healthy brain. *Plos One*. 2011; 6(7):e22193. [PubMed: 21829449]
19. Ecker C, et al. Investigating the predictive value of whole-brain structural MR scans in autism: A pattern classification approach. *Neuroimage*. 2010; 49(1):44–56. [PubMed: 19683584]
20. Elsenbruch S, et al. Visceral sensitivity correlates with decreased regional gray matter volume in healthy volunteers: a voxel-based morphometry study. *Pain*. 2014; 155(2):244–249. [PubMed: 24099953]
21. Farmer MA, et al. Brain Functional and Anatomical Changes in Chronic Prostatitis/Chronic Pelvic Pain Syndrome. *Journal of Urology*. 2011; 186(1):117–124. [PubMed: 21571326]
22. Gurvits TV, et al. Magnetic resonance imaging study of hippocampal volume in chronic, combat-related posttraumatic stress disorder. *Biological Psychiatry*. 1996; 40(11):1091–1099. [PubMed: 8931911]
23. Gwilym SE, et al. Thalamic Atrophy Associated With Painful Osteoarthritis of the Hip Is Reversible After Arthroplasty A Longitudinal Voxel-Based Morphometric Study. *Arthritis and Rheumatism*. 2010; 62(10):2930–2940. [PubMed: 20518076]
24. Jiang ZG, et al. Sex-Related Differences of Cortical Thickness in Patients with Chronic Abdominal Pain. *Plos One*. 2013; 8(9)
25. Kairys AE, et al. Increased Brain Gray Matter in the Primary Somatosensory Cortex is Associated with Increased Pain and Mood Disturbance in Interstitial Cystitis/Painful Bladder Syndrome Patients. *J Urol*.
26. Koikkalainen J, et al. Improved classification of Alzheimer's disease data via removal of nuisance variability. *Plos One*. 2012; 7(2):e31112. [PubMed: 22348041]
27. Kuchinad A, et al. Accelerated brain gray matter loss in fibromyalgia patients: premature aging of the brain? *J Neurosci*. 2007; 27(15):4004–4007. [PubMed: 17428976]
28. Labus JS, et al. Irritable bowel syndrome in female patients is associated with alterations in structural brain networks. *Pain*. 2014; 155(1):137–149. [PubMed: 24076048]
29. Landis JR, et al. The MAPP research network: design, patient characterization and operations. *BMC Urol*. 2014; 14(1):58. [PubMed: 25085119]
30. Lathe R. Hormones and the hippocampus. *Journal of Endocrinology*. 2001; 169(2):205–231. [PubMed: 11312139]
31. Mathias SD, et al. Chronic pelvic pain: Prevalence, health-related quality of life, and economic correlates. *Obstetrics and Gynecology*. 1996; 87(3):321–327. [PubMed: 8598948]
32. May A. Chronic pain may change the structure of the brain. *Pain*. 2008; 137(1):7–15. [PubMed: 18410991]
33. Michels L, et al. The somatosensory representation of the human clitoris: an fMRI study. *Neuroimage*. 2010; 49(1):177–184. [PubMed: 19631756]
34. Mordasini L, et al. Chronic pelvic pain syndrome in men is associated with reduction of relative gray matter volume in the anterior cingulate cortex compared to healthy controls. *J Urol*. 2012; 188(6):2233–2237. [PubMed: 23083652]
35. Mourao-Miranda J, et al. Classifying brain states and determining the discriminating activation patterns: Support Vector Machine on functional MRI data. *Neuroimage*. 2005; 28(4):980–995. [PubMed: 16275139]
36. Mugler JP 3rd, Brookeman JR. Three-dimensional magnetization-prepared rapid gradient-echo imaging (3D MP RAGE). *Magnetic Resonance in Medicine*. 1990; 15(1):152–157. [PubMed: 2374495]
37. Murphy DG, et al. Age-related differences in volumes of subcortical nuclei, brain matter, and cerebrospinal fluid in healthy men as measured with magnetic resonance imaging. *Arch Neurol*. 1992; 49(8):839–845. [PubMed: 1343082]
38. Neugebauer V, et al. The amygdala and persistent pain. *Neuroscientist*. 2004; 10(3):221–234. [PubMed: 15155061]

39. Orru G, et al. Using Support Vector Machine to identify imaging biomarkers of neurological and psychiatric disease: A critical review. *Neuroscience and Biobehavioral Reviews*. 2012; 36(4): 1140–1152. [PubMed: 22305994]
40. Peters KM, et al. Prevalence of pelvic floor dysfunction in patients with interstitial cystitis. *Urology*. 2007; 70(1):16–18. [PubMed: 17656199]
41. Pfefferbaum A, et al. A quantitative magnetic resonance imaging study of changes in brain morphology from infancy to late adulthood. *Arch Neurol*. 1994; 51(9):874–887. [PubMed: 8080387]
42. Ploghaus A, et al. Exacerbation of pain by anxiety is associated with activity in a hippocampal network. *Journal of Neuroscience*. 2001; 21(24):9896–9903. [PubMed: 11739597]
43. Pontil M, Verri A. Properties of support vector machines. *Neural Computation*. 1998; 10(4):955–974. [PubMed: 9573414]
44. Prado WA, Roberts MHT. An Assessment of the Antinociceptive and Aversive Effects of Stimulating Identified Sites in the Rat-Brain. *Brain Research*. 1985; 340(2):219–228. [PubMed: 4027651]
45. Puri BK, et al. Regional grey and white matter volumetric changes in myalgic encephalomyelitis (chronic fatigue syndrome): a voxel-based morphometry 3 T MRI study. *Br J Radiol*. 2012; 85(1015):e270–e273. [PubMed: 22128128]
46. Rodriguez-Raecke R, et al. Brain Gray Matter Decrease in Chronic Pain Is the Consequence and Not the Cause of Pain. *Journal of Neuroscience*. 2009; 29(44):13746–13750. [PubMed: 19889986]
47. Schmidt-Wilcke T, et al. Striatal grey matter increase in patients suffering from fibromyalgia - A voxel-based morphometry study. *Pain*. 2007; 132:S109–S116. [PubMed: 17587497]
48. Schneider F, et al. Subjective ratings of pain correlate with subcortical-limbic blood flow: An fMRI study. *Neuropsychobiology*. 2001; 43(3):175–185. [PubMed: 11287797]
49. Schweinhardt P, et al. Increased gray matter density in young women with chronic vulvar pain. *Pain*. 2008; 140(3):411–419. [PubMed: 18930351]
50. Seminowicz DA, et al. Regional Gray Matter Density Changes in Brains of Patients With Irritable Bowel Syndrome. *Gastroenterology*. 2010; 139(1):48–U82. [PubMed: 20347816]
51. Smallwood RF, et al. Structural brain anomalies and chronic pain: a quantitative meta-analysis of gray matter volume. *Journal of Pain*. 2013; 14(7):663–675. [PubMed: 23685185]
52. Tu CH, et al. Brain morphological changes associated with cyclic menstrual pain. *Pain*. 2010; 150(3):462–468. [PubMed: 20705214]
53. Ung H, et al. Multivariate Classification of Structural MRI Data Detects Chronic Low Back Pain. *Cerebral Cortex*. 2012
54. Valet M, et al. Patients with pain disorder show gray-matter loss in pain-processing structures: a voxel-based morphometric study. *Psychosomatic Medicine*. 2009; 71(1):49–56. [PubMed: 19073757]
55. Villarreal G, et al. Reduced hippocampal volume and total white matter volume in posttraumatic stress disorder. *Biological Psychiatry*. 2002; 52(2):119–125. [PubMed: 12114003]
56. Wager TD, et al. An fMRI-Based Neurologic Signature of Physical Pain. *New England Journal of Medicine*. 2013; 368(15):1388–1397. [PubMed: 23574118]
57. Younger JW, et al. Chronic myofascial temporomandibular pain is associated with neural abnormalities in the trigeminal and limbic systems. *Pain*. 2010; 149(2):222–228. [PubMed: 20236763]

**Summary Statement**

A preliminary classifier of brain structure was identified in chronic pelvic pain using a support vector machine learning algorithm suggesting distributed regional gray matter increases.

Author Manuscript

Author Manuscript

Author Manuscript

Author Manuscript



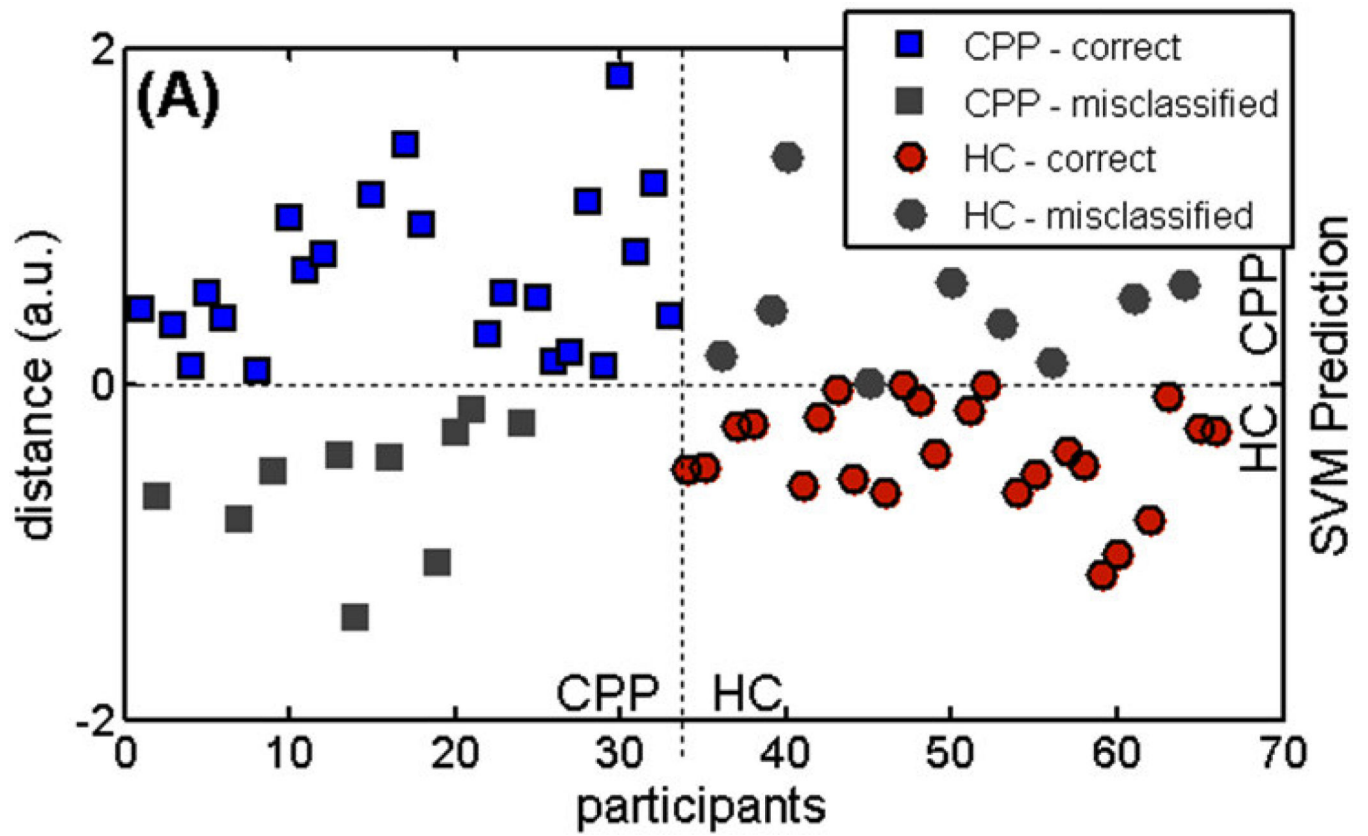


**Figure 1.** The distance in arbitrary units of each MR image from the trained SVM’s decision boundary (distance = 0) for individual participants with chronic pelvic pain (CPP) and individual healthy controls (HC). SVM prediction: positive distance is classified as CPP, while negative distance as HC. Grayed out data points are misclassified images.

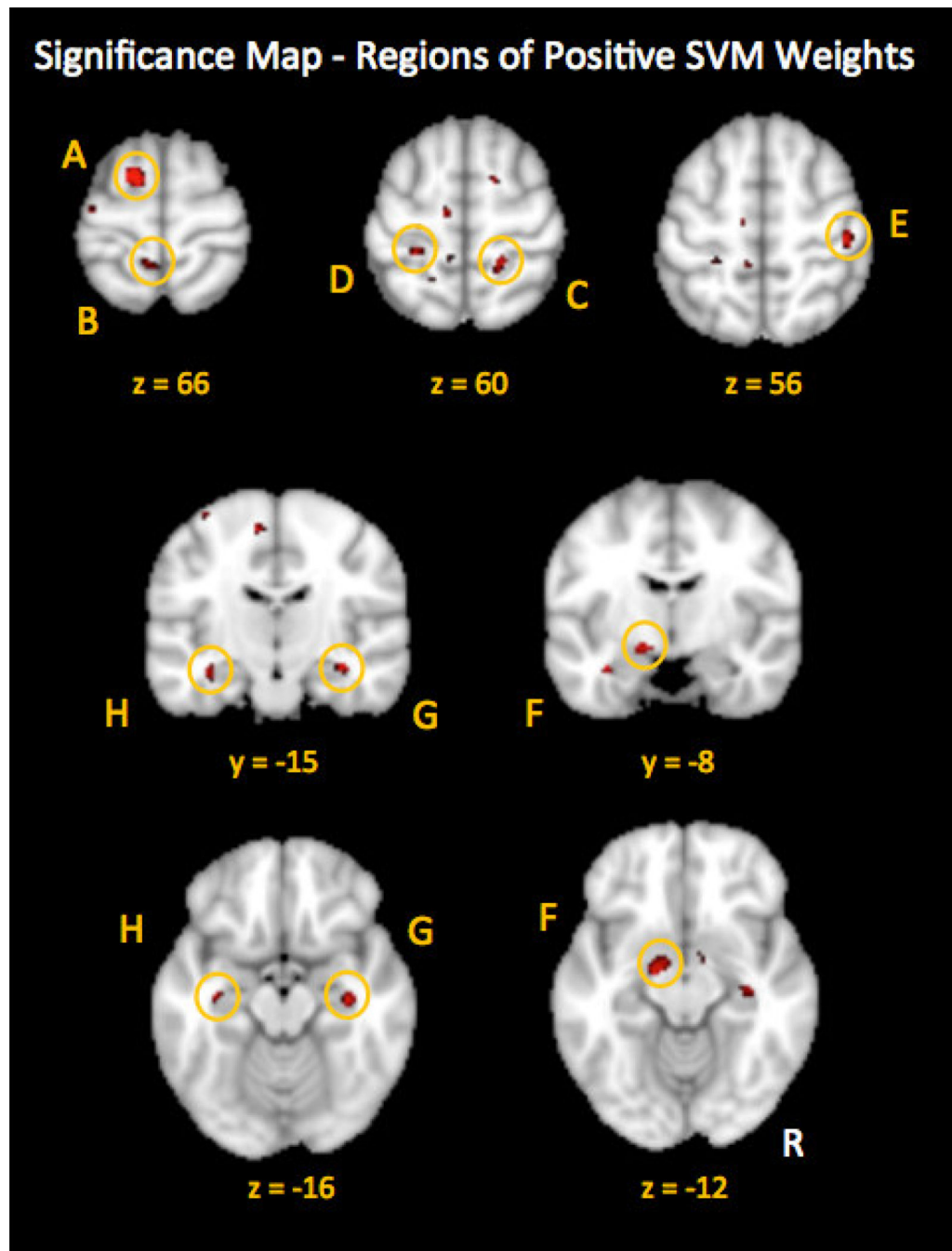


**Figure 2.**

Regions of positive SVM weight indicative of greater GM density in CPP as compared with HCs. Regions included the L. superior frontal gyrus / pre-supplementary motor area (A), L. postcentral gyrus / paracentral lobule (B), R. primary somatosensory cortex (C), L. primary somatosensory cortex (D) and R. lateral primary somatosensory cortex (E), L. parahippocampal gyrus / amygdala (F), R. parahippocampal gyrus / hippocampus (G), and L. parahippocampal gyrus / hippocampus (H). All regions were FDR-corrected for multiple comparisons ( $q < 0.05$ ); minimum cluster size = 20. (See Table 2 for details.)

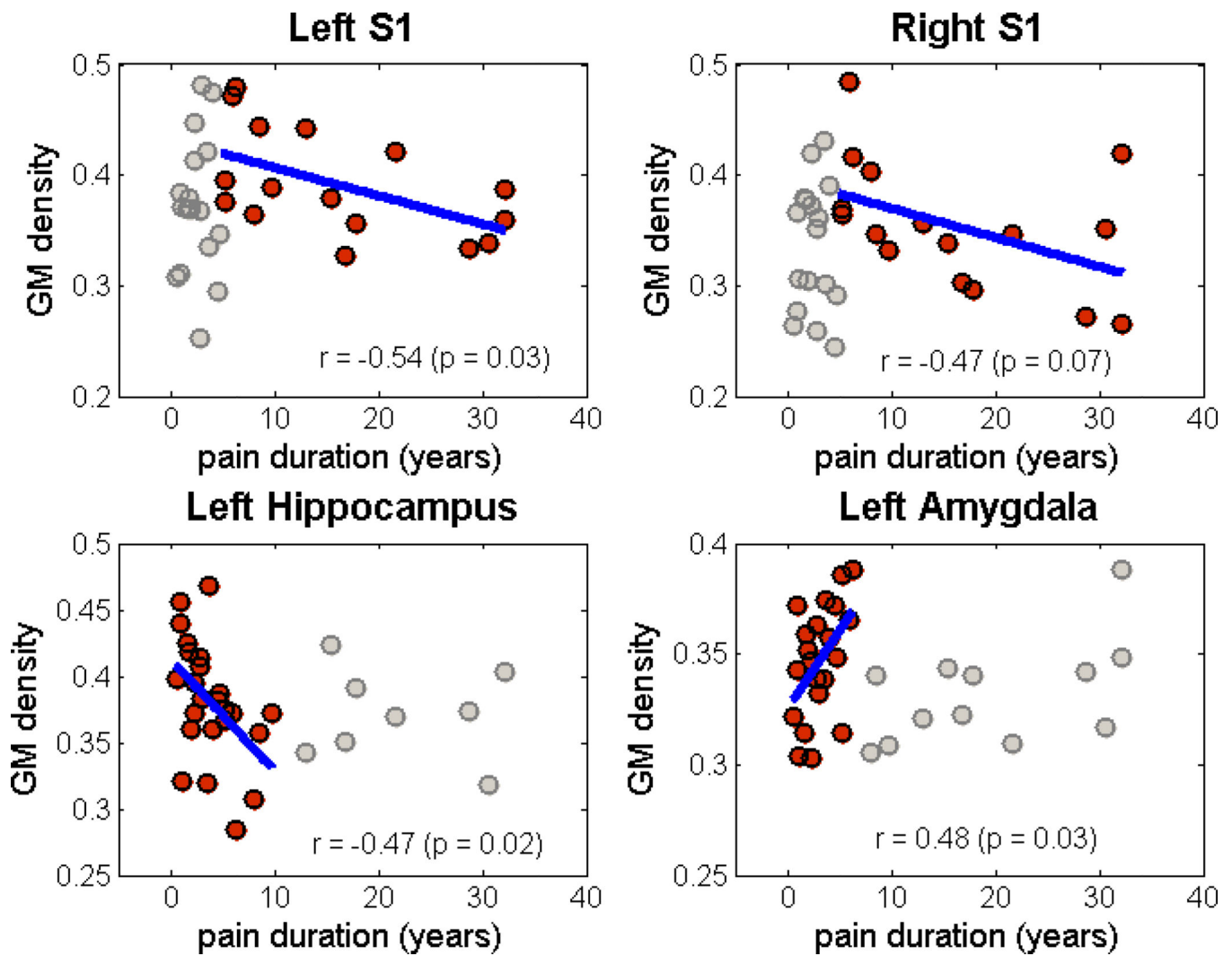


**Figure 3.**

Scatter plots showing correlation of GM density with pain duration in different stages of chronic pain (left S1 and right S1 for duration > 5 years, left hippocampus for duration < 10 years, and left amygdala for duration < 7.5 years, see Table 3). Gray points are outside the range of symptom duration where correlation was observed.

**Table 1**

Classification performance of the trained SVM

Measure	Value (%)	Significance, q
Accuracy	72.73	0.039
Sensitivity	69.70	0.067
Specificity	72.73	0.046
Positive predictive value	71.88	0.039
Negative predictive value	70.59	0.047

Author Manuscript

Author Manuscript

Author Manuscript

Author Manuscript

**Table 2**

Regions contributing to the classification performance of the trained SVM.

	<b>Regions from Significance Map</b>	<b>Peak Coordinates (MNI)</b>	<b>Cluster size # of voxels</b>	<b>Individual Region Accuracies (%)</b>
A	Left superior frontal gyrus/preSMA (BA 6)	-14, 2, 66	51	74.2
B	Left postcentral gyrus/paracentral lobule (BA 5)	-6, -44, 66	32	60.6
C	Right postcentral gyrus/S1 (BA 3)*	18, -40, 60	22	72.7
D	Left postcentral gyrus/S1 (BA 3)*	-26, -36, 60	23	72.7
E	Right postcentral gyrus/S1 (BA 3)	44, -24, 56	26	69.7
F	Left parahippocampal gyrus/amygdala	-16, -6, -14	42	63.6
G	Right parahippocampal gyrus/hippocampus	32, -20, -14	42	56.1
H	Left parahippocampal gyrus/hippocampus	-32, -12, -22	44	71.2

(\* Regions close to those activated during electrical clitoral stimulation [24].)

**Table 3**

Correlation of gray matter density with symptom duration

Region	Duration	No. participants	Pearson's correlation ( <i>p</i> -value)
Left S1	<= 5 years	17	0.1064 (0.6844)
	> 5 years	16	-0.5392 (0.0311)*
Right S1	<= 5 years	17	-0.0136 (0.9586)
	> 5 years	16	-0.4658 (0.0690)**
Left Hippocampus	<= 10 years	24	-0.4670 (0.0214)*
	> 10 years	9	0.0484 (0.9016)
Left Amygdala	<= 7.5 years	21	0.4786 (0.0282)*
	> 7.5 years	12	0.5343 (0.0735)

(\* significant correlation, \*\* moderate correlation)

Author Manuscript

Author Manuscript

Author Manuscript

Author Manuscript